Available online at www.sciencedirect.com
SCIENCE DIRECT®
Earth and Planetary Science Letters 243 (2006) 732–748
EPSL
www.elsevier.com/locate/epsl

The influence of weathering process on riverine osmium isotopes in a basaltic terrain

Abdelmouhcine Gannoun [a,*], Kevin W. Burton [a], Nathalie Vigier [a,b], Sigurdur R. Gíslason [c], Nick Rogers [a], Fatima Mokadem [a], Bergur Sigfússon [c]

[a] *Department of Earth Sciences, The Open University, Walton Hall, Milton Keynes, MK7 6AA, UK*
[b] *CRPG, 15 rue Notre-Dame des Pauvres, 54501 Vandoeuvre-lès-Nancy, France*
[c] *Institute of Earth Sciences, University of Iceland, Sturlugata 7, 101 Reykjavík, Iceland*

Received 8 September 2005; received in revised form 9 January 2006; accepted 10 January 2006
Available online 28 February 2006
Editor: H. Elderfield

Abstract

This study presents Os isotope and comprehensive major and trace element data for the dissolved load, suspended particulates and bedload for Icelandic rivers, draining predominantly basaltic catchments that range in age from historic to ca. 12 Ma. Hydrothermal waters and precipitation have also been analysed. Both Os and Re concentrations are greater in the suspended load than the bedload, while Re/Os ratios are lower, suggesting that both elements are concentrated in weathering resistant minerals. Despite this elemental fractionation the suspended particulates and bedload for each river yield indistinguishable $^{187}Os/^{188}Os$ isotope compositions that range from 0.136 to 0.292. In contrast, the dissolved load (<0.2 μm filtered) often possesses a significantly more radiogenic Os isotope composition than the corresponding suspended or bed load with $^{187}Os/^{188}Os$ ratios ranging from 0.15 to 1.04. The isotope and elemental data for the dissolved load can be explained in terms of an unradiogenic contribution from congruent basalt weathering (and/or hydrothermal input) and a radiogenic contribution that arises from two distinct processes. For the glacier-fed rivers there is a covariation between $^{187}Os/^{188}Os$ and the extent of glacial cover in the catchment, and this is most readily explained by the entrainment of seawater aerosols into precipitation and subsequent glacial melting. While for direct-runoff (and spring-fed rivers) there is a covariation between $^{187}Os/^{188}Os$ and the age of the bedrock in the catchment, that cannot be explained by congruent weathering of old basalt. Calculations indicate that those direct-runoff rivers with radiogenic $^{187}Os/^{188}Os$ values are also undersaturated with respect to the primary basalt minerals olivine, pyroxene and plagioclase, indicating that these phases are unstable and prone to preferential dissolution. Published Re–Os isotope data indicate that the same phases possess exceptionally high $^{187}Re/^{188}Os$ ratios and thus evolve to radiogenic $^{187}Os/^{188}Os$ compositions in very short time intervals. Taken together, these results indicate that incongruent (preferential) weathering of certain primary basalt minerals can impart a radiogenic Os isotope composition to the dissolved riverine load. Nevertheless, overall the Os isotope signal to the Oceans from Icelandic rivers is little affected because rivers with unradiogenic $^{187}Os/^{188}Os$ values and a high discharge dominate the Os flux.

Keywords: Re–Os isotopes; basaltic rivers; Iceland; weathering susceptibility; saturation state; incongruent weathering

* Corresponding author. Fax: +44 1908 655151.
E-mail address: a.gannoun@open.ac.uk (A. Gannoun).

0012-821X/$ - see front matter © 2006 Elsevier B.V. All rights reserved.
doi:10.1016/j.epsl.2006.01.024

1. Introduction

Understanding the relationship between global temperature and continental weathering potentially provides a fundamental insight into the processes that perturb the Earth's climate system. Rising temperature is thought to accelerate chemical weathering of silicates causing drawdown of atmospheric CO_2, which in turn leads to cooler temperatures through a reduced greenhouse warming [1,2]. Many natural radiogenic isotopes in seawater are sensitive to the variations in continental weathering and erosion that occur in response to climatic or tectonic change. The most widely used is strontium (Sr) and periods of increasing $^{87}Sr/^{86}Sr$ in seawater have been linked to intensified continental weathering caused by orogenesis [3] or glaciation [4]. However, many have questioned the utility of marine $^{87}Sr/^{86}Sr$ as a proxy for silicate weathering [5], and the long residence time of Sr in the oceans (3–4 Myr) means that short-term variations in input are not easily resolved [6]. Radiogenic isotopes with shorter residence times in the oceans, such as neodymium (Nd) or lead (Pb) (several hundred years) have the capability to respond to short-term variations in input [7], but it is unclear to what extent they reflect a geographically local response to climate or tectonic change, rather than a truly global signal. The osmium (Os) isotope composition of seawater reflects a balance of input from radiogenic continental material, and an unradiogenic signal from hydrothermal alteration of oceanic crust and the dissolution of particulate meteorite material [8,9]. The utility of Os as an oceanic tracer is that its residence time in the oceans is sufficiently short to respond, in phase, with short term fluctuations in input, but long enough for the signal to be global in extent [11,10]. Therefore, the system offers the capability to distinguish both high-frequency climatic and low-frequency tectonic events [12].

The principal control on the Os isotope composition of the continental crust is rock type and age. Differing rock types have distinct $^{187}Re/^{187}Os$ (parent/daughter) ratios and isotope compositions, and radiogenic ^{187}Os is produced over time. Thus, preferential weathering of very radiogenic or very old rocks has the potential to bias the continental signal towards more radiogenic values. The first measurements of Os isotopes in rivers suggested broadly congruent dissolution of bedrock [13,14]. However, more recent data for a number of rivers shows that in many cases the dissolved load is not in Os isotope equilibrium with the suspended load or bedload, and this has been attributed to incongruent weathering of mineral phases. It is well established from both natural systems and experimental study that different minerals have different weathering susceptibilities [15], and several radiogenic isotope systems, such as Hf and Pb in waters, may be dramatically affected by the preferential weathering of specific minerals [16,17]. Release of relatively radiogenic Os from glacial soils has been attributed to preferential weathering of biotite [18], consistent with much of the river data. In this case the interpretation of seawater Os isotope records may be hindered because it is not possible to distinguish changes caused by variations in the weathering flux from those caused by variations in the composition of weathered material or in the weathering process itself (i.e. changes in weathering congruence).

Basaltic rocks are highly susceptible to weathering [19] and consequently have a much greater effect on atmospheric CO_2 consumption than might be expected from their areal extent. For example, estimates for present-day CO_2 consumption due to silicate weathering suggest that between 30% and 35% may be attributable to basaltic rocks although basalts constitute less than 5% of the continental area [20]. Under normal circumstances weathering of young mantle-derived basalts will yield an unradiogenic Os isotope signal to the oceans, akin to that from hydrothermal input (e.g. [21]). However, recent work has shown that the constituent minerals of basalts, such as olivine or clinopyroxene, possess exceptionally high $^{187}Re/^{188}Os$ ratios, and consequently radiogenic ^{188}Os can be produced from the decay of ^{187}Re over very short periods of time (i.e. $\sim 10^6$ years or less) [22]. The very same phases are amongst the most susceptible to weathering (e.g. [15]), and thus it can be anticipated that incongruent weathering of basalt, even quite soon after eruption, may potentially yield a relatively radiogenic signal.

This study presents Os isotope data for dissolved, suspended and bed loads of rivers draining predominantly basaltic watersheds in Iceland. These watersheds are essentially monolithological, hence there is no significant effect from the weathering of different rock types. The basalts do however vary in age and thus it is possible to examine the relationship between the age of the basalt and the preferential weathering of constituent basalt minerals. The influence of rainwater and hydrothermal waters on the riverine Os isotope composition is also assessed.

2. Climate, geology and hydrology

Iceland lies close to the Arctic circle and the climate is oceanic boreal with cool summers and relatively warm winters. The mean temperature of the coastal areas and lowlands is around 4 °C, and the annual

precipitation varies from less than 400 mm to more than 4000 mm. The central region of Iceland consists of 500 to 700 m high plateau, with mountains up to 2000 m above sea level. Mountain ranges radiate in all directions from the central plateau separating valleys and dividing the coastal lowlands. The size of the island is about 103,000 km^2, which is about 0.1% of the global land area drained to the oceans. Glaciers in Iceland cover 11,260 km^2 or ~11% of the total area. Iceland was mostly covered by ice in the Pleistocene, but the ice caps attained their present size about 8000 years ago. By far the largest of these is Vatnajökull in SE Iceland with an area of 8300 km^2 and being up to 1000 m in thickness (equivalent in size to all the glaciers on mainland Europe).

The general features of the geology of Iceland are thought to be the result of a mantle plume, in addition to crustal accretion at the diverging lithospheric plates. Basaltic volcanic rocks are predominant (80% to 85%), the remainder being acidic intrusions and volcanoclastic sediments. The recent and upper quaternary volcanics are confined to the rift zone. As a result of crustal accretion, the age of the rocks generally increases with distance from the central rift zone (Fig. 1). The construction of Iceland began about 24 Ma but the oldest exposed rocks in the east and north-west of Iceland are 12.5 and 16.0 Ma, respectively [23].

Permeability is higher within the rocks of the young volcanic rift zone, and for this reason these areas have few surface streams. Compaction and sealing by secondary minerals reduces the permeability of the older rocks outside the active rift zones, and as a result surface runoff dominates in these areas. There is also a spatial variability in the hydrothermal activity in Iceland. High temperature activity, up to 300 °C occurs in the active rift zones, while low temperature activity, from ambient temperatures to about 150 °C, occurs in the older Quaternary and Tertiary areas.

The total annual discharge of the rivers in Iceland is 170 km^3, about 0.45% of the global river discharge to

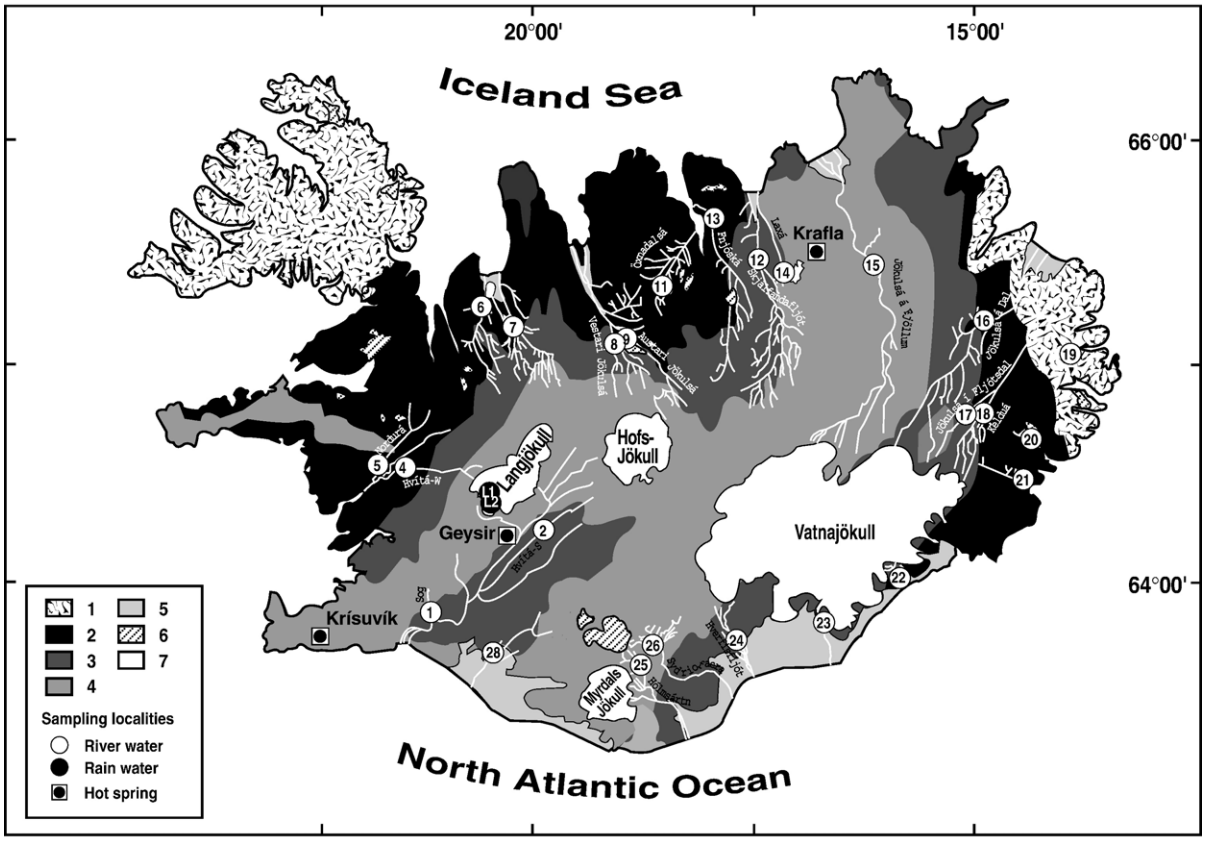

Fig. 1. Simplified geological map of Iceland after [24]: 1 = basic and intermediate extrusive rocks with intercalated sediments between 10 and 15 Myr; 2 = basic and intermediate extrusive rocks with intercalated sediments between 3.1 and 10 Myr; 3 = basic and intermediate extrusive rocks with intercalated sediments between 0.7 and 3.1 Myr; 4 = basic and intermediate lavas younger than 0.7 Myr; 5 = Holocene sediments; 6 = acid extrusives; 7 = glaciers. Sample type and localities are indicated in the legend.

the ocean. The annual flux of suspended load by Icelandic rivers (excluding glacier outburst floods) is 0.02 to 0.025 km^3 that is 0.3% of the global annual flux to the oceans [25]. The rivers in Iceland are usually classified as either spring-fed, glacier-fed or direct runoff, and mixtures thereof.

3. Field and analytical techniques

3.1. Sampling and storage

Twenty-five representative Icelandic rivers were sampled during late June and early July 2001 (Fig. 1). In the field, 15 l of river water were collected into precleaned (acid washed) containers. Samples were filtered through 0.2 μm cellulose acetate filters using a pressurized Sartorius® Teflon unit. Filtrate aliquots were acidified to a pH of 2 with ultra-pure nitric acid and stored in acid washed polypropylene (PP) bottles. The pH, temperature and alkalinity were determined in the field. The stability of Os over time in PP storage vessels has been demonstrated previously [26]. Where possible, suspended particulate material was recovered from the acetate filters and bed load was also collected for analysis. In order to characterise the Os input to surface waters from atmospheric precipitation, two precipitation samples were collected from Lanjokull glacier (at 1100 m elevation, 64°35′ N, 20°20′W), and three thermal spring water samples (Fig. 1) from the rift zone (Krafla, Geysir and Krísuvík) were also investigated.

3.2. Anions, cations and trace elements

The anion concentrations in the dissolved load were measured by ion chromatography, with an uncertainty of ±1–3% (1σ). Cation concentrations were measured by ICP-MS. Major elements were calibrated against a set of synthetic multi-elemental standards prepared gravimetrically from high purity single element standard solutions. The trace element composition of an internal standard (Scottish river water, SCO 2/15) and the river water samples were then calibrated against this standard. The accuracy of the analysis was assessed by running the natural water certified reference material SLRS4. Sands were finely powdered and dissolved by an acid attack (HF, HNO_3, HCl). When the digestion was not completely achieved, $HClO_4$ was also used. The following certified reference materials were used for external calibration: BHVO-1, BIR-1, JB-2, UBN. BHVO-1 was used as a monitoring standard for each batch of measurements. The external error determined from the repeated analyses of the rock standards is usually better than 3% (1σ) for all elements that have concentrations >0.25 ppm.

3.3. Re–Os analysis

3.3.1. Filtered river, rain and hot spring water

The technique for the chemical separation of Os used in this study follows that originally developed by Birck et al. [27] and later modified for natural waters [11,26]. In brief, 60 ml of water is introduced into 120 ml savillex® PFA-Teflon pressure vessel together with Br_2–40%CrO_3–H_2SO_4 (2:1:1 ml) and ^{190}Os enriched tracer. The pressure vessel is then closed and heated to 90 °C in the oven for 72 h. This 'hot' oxidation technique achieves complete spike-sample homogenisation and the conversion of all Os species present to OsO_4. Osmium is then extracted from the water into liquid bromine [26]. The hexabromo–osmate fraction is then dried and purified using micro-distillation [26]. The total procedural blank for water chemistry during the course of this study was 0.017±0.003 pg, with a weighted mean $^{187}Os/^{188}Os$ of 0.266±0.040 (n=8). This blank accounts for between 1% and 22% of the total Os present in the samples, except for rainwater samples in which this proportion was 32%.

3.3.2. Oxidation duration

An oxidation experiment was undertaken to determine the duration of the oxidation step necessary to achieve complete tracer-sample equilibration. A sequence of test measurements on the Icelandic river sample IS 15 (Jökulsá á Fjöllum) is summarised in Fig. 2.

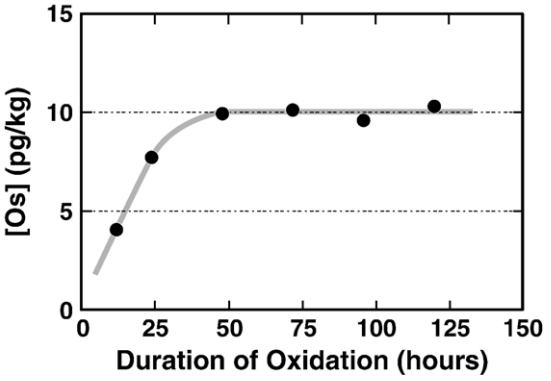

Fig. 2. Plot of the osmium content ([Os] pg/kg) versus the duration of the oxidation step (in hours) for the dissolved river water sample IS 15 (Jökulsá a Fjöllum). This step ensures isotopic equilibration between water sample and ^{190}Os tracer isotope. The kinetics are slow and require oxidation of Os to OsO_4 in a closed system at 100 °C. The plateau is reached after 48 h and the duration of oxidation was fixed at 72 h for all samples.

At least 48 h was necessary for the Os concentration to reach a plateau (cf. [11]). For all water samples analysed in this study, the duration of the oxidation was fixed at 72 h.

3.3.3. Suspended and bed load

The detailed analytical procedure for silicates has been reported elsewhere [27]. Approximately 0.4 g of bed load and between 10 and 40 mg of suspended load were crushed using an agate mortar. The powder is spiked using a mixed ^{190}Os–^{185}Re spike and then dissolved with HBr+HF in a 6 ml-savillex® teflon bomb at 150 °C. This step is followed by oxidation of Os using Br_2–CrO_3–HNO_3. Os is then extracted in liquid bromine, dried and further purified by micro distillation. The liquid left after Os extraction is reduced by ethanol and Re is extracted and purified by liquid/liquid extraction with isoamylic alcohol and 2 M HNO_3. Both Re and Os samples were analysed on platinum filaments as OsO^{3-} and ReO^{4-} oxides using negative thermal ionisation mass spectrometry (N-TIMS) [28,29] using the ion counting electron multiplier on a Thermo Finnigan Triton.

The total procedural blank for for Os for silicate analysis was 0.032±0.010 pg (n=7) with $^{187}Os/^{188}Os$ of 0.230±0.053. The Re blank ranged between 2.5 and 5 pg (n=12) with mean value of 3.5 pg (period from December 2002 to May 2003). $^{187}Os/^{188}Os$ of 0.1 pg Os JM standard was 0.1742±0.0010 (n=5), 0.1738±0.0009 (n=10) for 0.5 pg standard, 0.17420±0.00061 (n=5) for 1 pg and 0.173978±0.000048 (n=24) for the 14 pg standard. All values are indistinguishable within error from the published data for the same standard [31,30] and from the mean value from Faraday cup measurement on large standards (0.173946±0.000004 on 5–10 ng, n=16).

4. Results

4.1. Suspended and bed load

The Re and Os isotopic data of suspended load and bed load are given in Table 1. Rhenium abundances

Table 1
Rhenium and osmium isotope data for the suspended and bed loads of the Icelandic rivers

Sample	River name	Bed load				Suspended load			
		$^{187}Os/^{188}Os$	Os (ppt)	Re (ppt)	$^{187}Re/^{188}Os$	$^{187}Os/^{188}Os$	Os (ppt)	Re (ppt)	$^{187}Re/^{188}Os$
IS 1	Sog	0.1565±0.0030	30.92	949	150				
Rep.		0.1432±0.0005	26.32	670	124				
IS 2	Hvítá — S	0.1812±0.0026	13.72	716	256	0.1755±0.0022	52.3	998	93.6
Rep.		0.1675±0.0007	34.93	723	101				
IS 4	Hvítá — W	0.1403±0.0004	20.86	708	166				
IS 5	Nordurá	0.2326±0.0011	10.65	650	301				
IS 8	Vestari Jökulsá	0.1726±0.0010	22.59	1372	298				
IS 9	Austari Jökulsá	0.1365±0.0006	18.27	995	265				
Rep.		0.1404±0.0013	29.69	1066	175				
IS 11	Öxnadalsá	0.1555±0.0007	34.31	316	45				
IS 12	Skjálfandafljót	0.1751±0.0062	18.25	1318	354	0.1753±0.0018	46.19	1737	184
IS 13	Fnjóská					0.2168±0.0015	35.64	1923	266
IS 14	Laxá	0.1385±0.0007	18.83	1818	471				
IS 15	Jökulsá á Fjöllum	0.1615±0.0009	8.965	1400	764	0.1654±0.0009	18.88	2828	734
IS 16	Jökulsá á Dal					0.1471±0.0030	26.71	685	125
IS 17	Jökulsá í Fljótsdal	0.1471±0.0008	9.855	535	265	0.1540±0.0008	16.42	600	179
IS 18	Kelduá	0.1813±0.0009	3.654	732	982	0.1897±0.0028	13.27	1577	583
Rep.		0.1909±0.0009	5.969	741	609				
Is 21	Geithellnaá	0.2503±0.0009	7.517	603	397				
IS 22	Steinavötn					0.2927±0.0066	22.3	2267	506
IS 23	Skaftafellsá					0.1540±0.0026	15.24	560	179
IS 24	Hverfisfljót	0.1375±0.0009	6.85	1464	1042	0.1332±0.0012	14.28	1267	433
IS 25	Hólmsárvatn	0.2478±0.0008	4.207	1444	1698				
IS 26	Sydri-Ófaera	0.1981±0.0008	4.831	1218	1239				
Rep.		0.2145±0.0007	7.135	1234	852				
IS 28	Raudilaekur					0.2499±0.0029	10.4	849	404

All errors are $2\sigma_{mean}$, $^{187}Os/^{188}Os$ are normalised to $^{192}Os/^{188}Os$=3.08271 [32] and corrected using measured $^{18}O/^{16}O$ and $^{17}O/^{16}O$ ratios of 0.002047 and 0.00037, respectively. Replicate measurements (Rep.) are for the same split powder repeated through both chemistry and mass spectrometry.

in the bed and suspended loads range from 300 to 1820 and from 560 to 2900 ppt, respectively. While Os concentrations show a small range from 3.6 to 52 ppt. The suspended load always possesses a higher Re and Os concentration than the corresponding bedload. Moreover, the Os enrichment from bedload to the suspended load is always greater than the relative Re enrichment, consequently, $^{187}Re/^{188}Os$ ratios for the bedload are always greater than the suspended load.

The $^{187}Os/^{188}Os$ ratio of the suspended and bedloads range from 0.13 to 0.29 and from 0.13 to 0.25, respectively. Despite the elemental fractionation between both phases, the Os isotope composition of suspended and bed loads is indistinguishable (for those samples for which both were measured; Fig. 3). Some of the more radiogenic values are higher than those previously observed for Icelandic basalts, although most of the existing data are for basalts from the young active zone [33–35] in which little radiogenic growth of ^{188}Os is likely to have occurred.

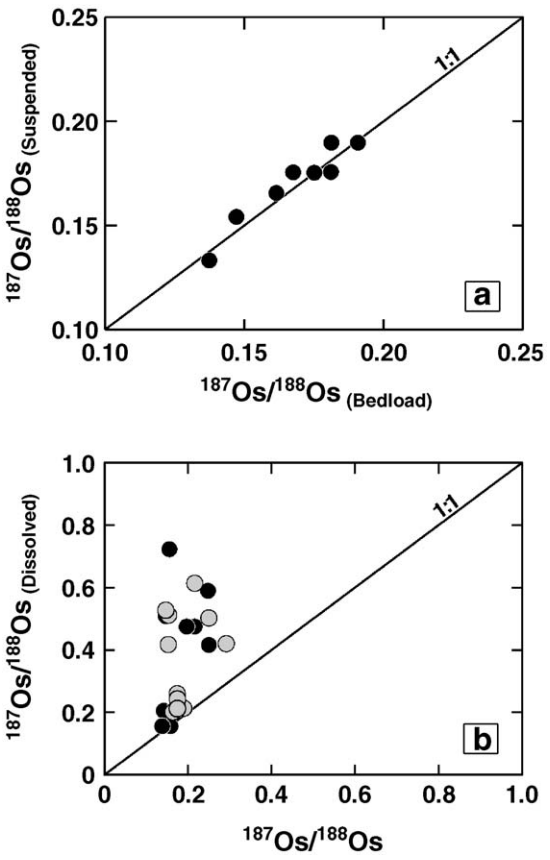

Fig. 3. Osmium isotope systematics in dissolved, suspended and bed load. (a) Despite the fractionation of Re and Os between suspended and bed load, the Os isotope composition remains similar. (b) In contrast, in almost all cases the $^{187}Os/^{188}Os$ for the dissolved load is more radiogenic than the corresponding suspended (black circles) and/or bed load (gray circles).

4.2. Dissolved phase

The Os concentration and isotope composition measured in filtered river waters is given in Table 2. Dissolved Os concentrations ($n=25$) range over an order of magnitude from 1 to 20 pg/kg, while $^{187}Os/^{188}Os$ isotope ratios range from 0.15 for Hvita-W (IS 4) to 1.04 for the Heidarvatn river (IS 19). All of these values are less radiogenic than the seawater value (~1.06 [11]) and the estimated riverine global average ($^{187}Os/^{188}Os=1.54$ [26]). The most radiogenic value was obtained for the river draining the oldest basalt in the eastern part of Iceland, while the lowest $^{187}Os/^{188}Os$ isotope ratios were observed for rivers draining the central active zone. Most significantly in almost all cases the $^{187}Os/^{188}Os$ ratios for the dissolved phase is more radiogenic than the corresponding suspended and/or bed load, in some instances significantly so (Fig. 4).

4.3. Precipitation and geothermal water

Osmium isotope and other elemental data for precipitation and geothermal water samples are given in Table 1. A detailed description of the chemistry of precipitation in Iceland is given elsewhere [25]. Chlorine concentrations for the samples analysed here range from 1.36 to 1.63 ppm which places them at the lower end of the range reported for Iceland (0.3 to 118 ppm, with an average of 9 ppm [25]). The X/Cl molar concentration ratios for Mg, Na, K, Ca, Sr are 0.093, 0.9, 0.003, 0.02, 0.0002, respectively, which points to a predominantly oceanic origin. Osmium concentrations in the two precipitation samples are below the range observed for river water (0.56 and 0.69 pg/kg) and below the values reported for rain from the Azores and Reunion [26] (7.6 and 14.7 pg/kg, respectively). The Os/Cl molar ratio for seawater is about 10^{-13} [36,11] and if the Os in the rain is solely marine, typical concentrations of 7 and 8 fg/kg are then expected, about 100 times lower than the concentrations observed here.

The $^{187}Os/^{188}Os$ isotope ratios for rainwater (ranging from 0.15 to 0.19) are however much lower than seawater but similar to those reported previously for rainwater from the basaltic islands of the Azores (0.17) and Réunion (0.18) [26]. Thus, despite the oceanic origin indicated for major elements, the unradiogenic

Table 2
Osmium isotope data and chemical compositions of the dissolved loads of Icelandic rivers

Sample	River name	T (°C)	pH	$^{187}Os/^{188}Os$ [a]	[Os] (pg/kg)	[^{188}Os] (pg/kg)	Na [b] ppm	Mg [b] ppm	Ca [b] ppm	K [b] ppm	Al ppm	Mn ppb	Rb ppb	Sr ppb	Ba ppb	Cl ppm	SO_4 [b] ppm	NO_3 ppm	Area (km^2)	Age (Myr)	Glaciers (%)	Mean discharge (km^3/yr)
River water																						
IS-1	Sog	7.7	7.78	0.157±0.002	10.6	1.38	8.09	1.33	4.27	0.61	12.01	2.23	0.73	5.36	0.12				439	0.27	0	3.18
IS-2	Hvítá- S	9.5	8.04	0.208±0.006	9.91	1.29	6.67	1.27	4.1	0.56	39.48	2.24	0.49	5.09	0.16	3.30	4.55	0.35	1987	0.67	21	3.45
IS-4	Hvítá-W	5.0	7.65	0.156±0.002	12.7	1.66	6.26	0.94	2.9	0.4	47.98	1.54	0.52	4.00	0.15	4.18	1.85	0.15	970	1.22	9	2.52
IS-5	Nordurá	7.8	7.93	0.244±0.005	3.21	0.42	5.60	1.39	3.45	0.31	5.89	2.43	0.31	6.12	0.15	7.86	1.95	0.28	391	5.90	0	0.64
IS-6	Vididalsá	8.7	8.03	0.403±0.006	2.88	0.37	7.12	3.55	6.32	0.77	3.39	11.84	1.01	17.22	0.24				445	4.13	0	0.24
IS-7	Vatnsdalsá	8.9	8.12				8.67	2.51	5.13	1.09	9.28	1.8	1.05	10.79	0.29	6.32	1.62		643	1.88	0	0.28
IS-8	Vestari Jökulsá	7.9	7.61	0.253±0.004	8.56	1.10	7.99	4.13	4.99	1.14	19.78	0.66	1.11	6.98	0.21	2.81	2.04	0.35	815	2.43	12	0.66
IS-9	Austari Jökulsá	7.3	7.70	0.204±0.003	5.21	0.68	4.36	0.52	2.48	0.35	35.2	0.45	0.38	2.13	0.05	1.39	0.73	0.16	965	2.86	16	1.08
IS-11	Öxnadalsá	7.5	7.50	0.702±0.012	1.86	0.22	2.16	0.7	2.14	0.31	6.99	0.44	0.36	5.16	0.15	2.10	0.58	0.15	74	5.90	0	
IS-12	Skjálfandafljót	8.0	7.68	0.256±0.007	9.30	1.20	6.99	1.72	4.49	0.48	26.24	1.72	0.5	5.24	0.14	2.23	3.41	0.14	2428	1.29	0	2.34
Rep.		8.0	7.68	0.240±0.006	8.66	1.12																
IS-13	Fnjóská	8.0	7.38	0.610±0.009	1.64	0.20	3.00	0.81	2.79	0.25	8.41	1.41	0.26	2.08	0.11				981	7.90	0	1.28
IS-14	Laxá	11.0	9.08	0.148±0.004	20.5	2.71	20.1	3.40	6.59	1.24	20.6	1.34	1.52	9.36	0.17	3.74	16.1	0.25	81	0.01	0	1.16
IS-15	Jökulsá á Fjöllum	10.0	7.95	0.197±0.006	9.92	1.29	11.01	1.64	4.22	0.59	28.16	0.83	0.47	4.67	0.10				5179	0.30	21	5.17
IS-16	Jökulsá á Dal	6.0	7.20	0.524±0.010	1.82	0.23	3.27	0.79	3.87	0.21	35.5	2.54	0.16	1.79	0.10				3321	1.71	43	4.43
IS-17	Jökulsá í Fljótsdal	5.5	7.46	0.508±0.010	1.16	0.14	2.73	0.84	6.46	0.19	21.35	5.64	0.12	4.89	0.05	1.35	2.51	0.08	558	2.14	26	1.02
IS-18	Kelduá	5.3	7.68	0.211±0.004	15.0	1.94	1.55	0.74	1.83	0.14	8.86	0.83	0.15	3.19	0.09	1.96	0.55	0.35	398	4.89	6	0.71
IS-19	Heiorratn	3.7	7.18	1.041±0.009	1.55	0.18	2.87	0.87	2.00	0.16	7.91	1.55	0.12	3.61	0.12				46	11.20	0	0.13
IS-20	Fossá	7.4	7.59	0.567±0.012	2.20	0.27	2.47	0.65	1.59	0.1	2.37	0.51	0.08	2.81	0.03				74	5.90	0	0.25
Rep.		7.4	7.59	0.580±0.011	1.87	0.23																
IS-21	Geithellnáá	7.4	7.61	0.416±0.008	1.20	0.15	2.40	0.67	1.98	0.14	7.28	0.53	0.12	3.02	0.06	3.00	0.91	0.07	184	5.90	11	1.04
IS-22	Steinavötn	9.1	7.62	0.418±0.007	2.86	0.36	3.85	0.84	13.5	0.09	28.5	1.16	0.07	6.10	0.04	3.94	12.9	0.17	111	0.57	100	
IS-23	Skaftafellsá	1.7	9.19	0.415±0.002	1.01	0.13	5.51	0.32	10.27	0.33	299.7	8.57	0.29	4.28	0.59	3.26	1.72		208	1.66	44	1.26
IS-25	Hólmsártn	8.7	7.56	0.590±0.009	1.78	0.22	5.64	1.1	3.21	0.48	11.18	2.93	0.56	8.32	0.07	2.77	2.80	0.10	122	0.21	100	2.97
IS-26	Sydri-Ófaera	8.7	6.94	0.475±0.009	3.45	0.43	7.51	0.95	3.63	0.38	16.2	0.60	0.24	5.13	0.51	3.20	3.07	0.31	71	0.28	25	
IS-27	Ytri-Rangá	8.0	8.48				22.48	5.28	10.38	1.33	6.81	4.70	0.95	34.3	0.21	10.82	15.8	0.36	244.9	0.86	0	1.39
IS-28	Raudilaekur	10.0	6.97	0.499±0.007	2.02	0.25	16.31	12	19.96	1.45	5.59	406	1.95	79.85	0.55	14.28	4.47	0.28	21	3.17	0	
Rainwater																						
O2-L1	Langjökull			0.151±0.006	0.69	0.090	0.81	0.083	0.028	0.002		0.16		0.54	0.024	1.36	0.25	0.47				
O2-L2	Langjökull			0.194±0.014	0.56	0.072	0.99	0.11	0.034	0.007		0.082		0.67	0.034	1.63	0.32	0.06				
Rep.				0.189±0.004																		
Geothermal water																						
#1	Krafla			0.160±0.002	21.5	2.80	0.42	1.43	2.34	0.39	2.56	85.5										
Rep.	Krafla			0.162±0.008	22.7	2.97	0.41	1.41	2.36	0.39	2.47	85.1										
#2	Geysir			0.175±0.004	19.1	2.49																
#3	Krísuvík			0.169±0.002	17.5	2.28																
Rep.	Krísuvík			0.173±0.005	17.9	2.35																

[a] See Table 1 footnote and the main text for calculation, normalisation and blank correction.

[b] River waters are corrected from atmospheric input using Cl concentrations and oceanic X/Cl ratio (X for the given element) and assuming that all Cl of the dissolved load has an atmospheric origin.

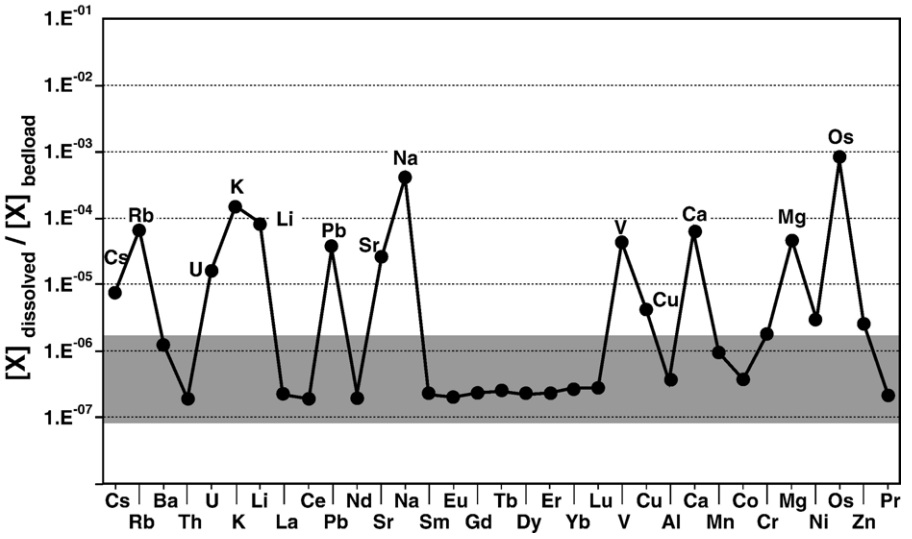

Fig. 4. Extended pattern of trace and major element partitioning between the dissolved-load and the bedload. The pattern represents the average of 15 Icelandic rivers. Bedload elemental data are given in the supporting online material. The shaded area corresponds to the diluted bedrock composition which serves to identify the mobile elements which are relatively enriched in the dissolved load. As shown, Os can be considered amongst the most soluble elements.

$^{187}Os/^{188}Os$ isotope composition implies a local source for the Os.

Geothermal water samples possess Os concentrations ranging from 17 to 23 pg/kg which are higher than those obtained for river or rainwaters. The $^{187}Os/^{188}Os$ ratios range from 0.16 to 0.18 and are similar to the rain and within the range obtained for the suspended and bed load. This distribution is consistent with the chemistry of the thermal springs being largely controlled by temperature and water/rock interaction. There is no evidence for seawater percolation on the studied samples despite the fact that the source at Krísuvík is associated with the active volcanic zone close to the coast.

5. Discussion

5.1. Re–Os isotope and elemental variations

Rhenium and Os concentrations in the bedload are typical of those found in oceanic basalts. The range of concentrations is slightly larger than those previously published for Icelandic basalts. However, these samples were largely picritic [33–35] and while this makes them more amenable for measurement using higher blank chemical techniques they are unlikely to be representative of the catchments studied here. Elemental data indicate that the suspended load always possesses higher concentrations of both Re and Os than the corresponding bedload. The enrichment of Os in the suspended load is always greater than that of Re. This relative difference in behaviour between Re and Os results in the $^{187}Re/^{188}Os$ of the bedload being always higher than that of the suspended load. Despite this difference in the $^{187}Re/^{188}Os$ ratio there is no significant difference in the radiogenic isotope composition ($^{187}Os/^{188}Os$) of the suspended load and corresponding bedload, at least for those samples for which both have been measured. Thus, assuming that both suspended and bedload were ultimately derived from the same bedrock, then this suggests that the differential enrichment of Re and Os in the suspended load must have occurred relatively recently. The relative enrichment of Re and Os in the suspended load discussed above, can not be directly related to the thermodynamic solubility of the both elements in aqueous environments, despite the fact that such an approach can be applied to the most of major and trace elements being partitioned between silicate phases. In this case, however, the relative Re and Os enrichment relates simply to the fact that both elements are concentrated in the weathered fine fraction. Os is a platinum group element (PGE) which are usually concentrated in accessory phases (such as sulphides or alloys). Fig. 4 shows major and trace element concentrations in the dissolved load normalised to the bed load composition. Osmium is amongst the most soluble elements (similar to Rb, K, Sr...) and this is consistent with the presence of Os as soluble oxyanions in natural waters.

5.2. Osmium isotope and elemental variations in the dissolved load

The Os isotope ratio of the dissolved load shows a range that is four times greater than that observed in the suspended or bed load (Fig. 3). When illustrated on a mixing diagram (Os isotope composition against the reciprocal of the concentration) all the data (Fig. 5), with the exception of sample IS 19, fall within a field delimited by three potential end-members, seawater, rainwater and an unradiogenic end-member (low $^{187}Os/^{188}Os$ and high Os content) of basaltic origin. Most of the data in Fig. 5 show a positive covariation, and hence mixing could be explained as occurring in two stages. The first, where a common radiogenic component comprises a mixture of rainwater and seawater (~9% seawater and ~91% rainwater yielding a $^{187}Os/^{188}Os$ ratio of ~0.65–0.75). In practice, this would constitute rainwater which has entrained aerosols carrying the Os isotope composition of seawater. The second stage, would then involve the mixing of this radiogenic component with basalt derived unradiogenic Os.

It is tempting then to attribute the entire range of Os isotopes seen in the dissolved load of Icelandic rivers as being simply due to the involvement of a rainwater–seawater mix and a basaltic contribution (through basalt weathering or hydrothermal waters). However, Cl and Na concentrations in the dissolved load are low, and there is no covariation with Os as might be expected from a seawater contribution. Although this assumes that the speciation and behaviour of Cl, Na and Os is the same in these river waters. More importantly direct addition of rainwater is unlikely to explain the observed variations because the geographical variation in the $^{187}Os/^{188}Os$ of the rivers does not match the pattern of rainfall variations seen across Iceland. Neither does it match the seawater contribution to precipitation, where the Cl content of rainwater shows a strong gradient across Iceland, from values greater than 40 ppm in south-eastern coastal areas to less than 1 ppm in the central highlands. Thus it might be expected that rivers in the south-eastern coastal areas would possess more radiogenic Os isotope compositions, but this is not the case.

An alternative possibility is that of an indirect contribution from rainwater via glacial meltwater. Examination of sample proximity to major glaciers, such as Vatnajokull (Fig. 1) shows that many glacier-fed rivers possess radiogenic $^{187}Os/^{188}Os$ isotope compositions (Fig. 5). The effect from glacial meltwater is more

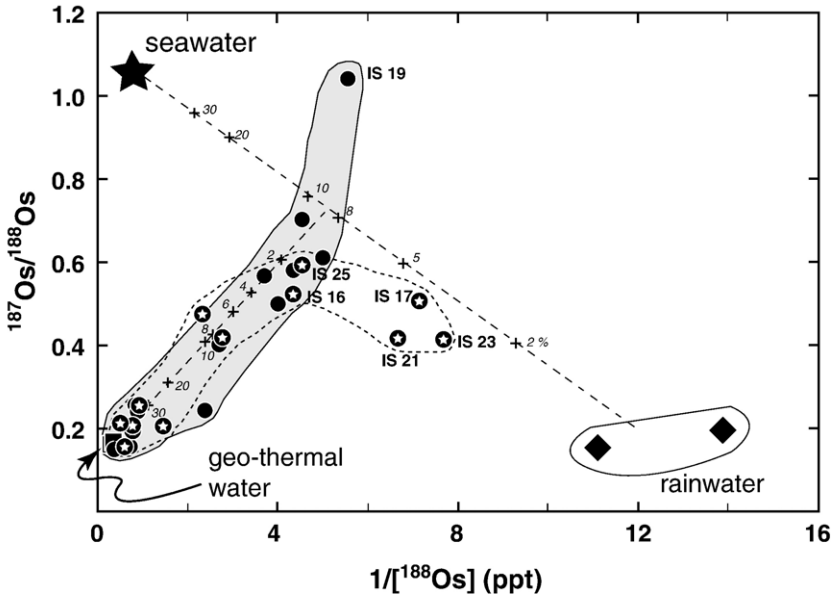

Fig. 5. Dissolved osmium isotope composition against the reciprocal of the concentration. The filled circles represent rivers without a glacial contribution in their catchments; the circles with stars represent rivers with a glacial contribution. Geothermal-, rain- and seawater can be considered as end-members. The data show a broad positive covariation (R^2=0.91), which could be expressed by ternary mixing occurring in two stages. The first stage, where a common radiogenic component comprises a mixture of rainwater and seawater (~10% seawater, ~90% of rainwater) yielding a $^{187}Os/^{188}Os$ ratio of ~0.7. The second stage, would then involve the mixing of this radiogenic component with basalt derived unradiogenic Os in varying proportions. Three glacial rivers do not lie on this positive trend and likely reflect a greater contribution from rainwater. Dashed lines are mixing lines and figures (in italic) on the marks represent proportion (in percent) of the one of the end-members. For "rainwater–seawater" line, figures are those of seawater proportion; for the other line, figures are those of the unradiogenic component involved in the mixture.

clearly illustrated in Fig. 6 where the $^{187}Os/^{188}Os$ of the dissolved load is shown against the estimated percentage of glacial cover in the catchment. It is important to note that the percentage of glacial cover may not directly equate to meltwater contribution to the river. Nevertheless, in general, those rivers with a higher percentage of glacial cover do possess more radiogenic $^{187}Os/^{188}Os$ isotope compositions, and this is most likely explained by the entrainment of seawater derived Os in the glacial water. On Fig. 5 three of the glacier-fed rivers with the lowest Os concentrations are clearly displaced towards the rainwater end-member. However, other glacier-fed river samples with higher Os concentrations lie on an indistinguishable trend to that of the direct-runoff rivers.

For the direct-runoff rivers the sample with the most radiogenic $^{187}Os/^{188}Os$ isotope composition (not easily explained by seawater addition) also drains the oldest catchment, with an estimated average age of 11.2 Myr.

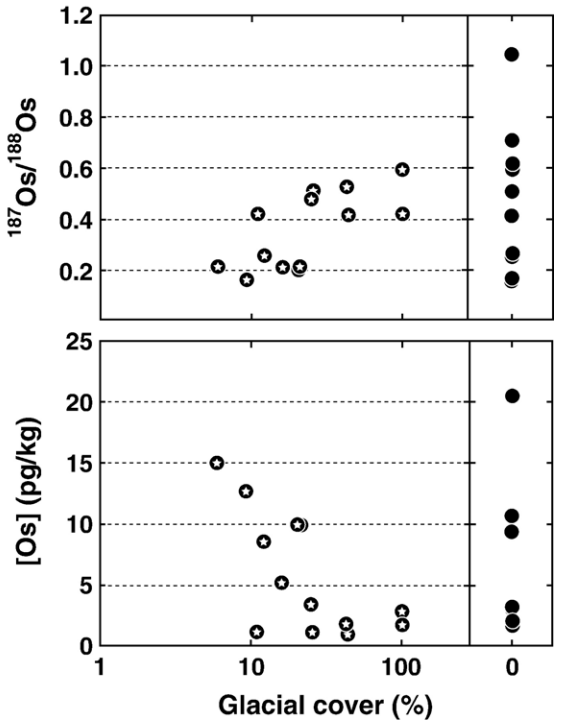

Fig. 6. Dissolved osmium isotope composition versus the glacial cover (as percent) in the river catchment. The box on the right side of the both plots, shows Os data from non-glacial rivers for comparison. Broad correlations are shown between the osmium isotope systematics and the glacial cover of the drainage basins expressed as percentage. Rivers draining areas with a high glacial cover seem to carry less dissolved osmium but that present has a radiogenic isotope composition. Some of those values can be attributed to weathering of relatively old basalt but others draining relatively young catchment areas are likely to acquire their radiogenic composition from seawater–rainwater contamination.

This relationship between $^{187}Os/^{188}Os$ and catchment age appears to hold for all the direct-runoff rivers, and there is positive covariation where the more radiogenic $^{187}Os/^{188}Os$ values are found in the older catchments (Fig. 7). In contrast, while some of the glacier-fed rivers may lie on this trend many do not, and in particular the most radiogenic $^{187}Os/^{188}Os$ seen is in a glacial rivers that drains a very young catchment, less than 1 Myr old (Fig. 7).

Taken together, these observations suggest that both glacier-fed and direct-runoff rivers sample an unradiogenic $^{187}Os/^{188}Os$ contribution characterised by higher Os concentrations that is most likely controlled by basalt weathering (or in some cases a contribution from hydrothermal water). However, there are two distinct processes that impart a radiogenic Os isotope composition to the dissolved load of many of the rivers. The first, affecting glacier-fed rivers is derived from an indirect seawater contribution via precipitation and subsequent glacial melting. The second, that affects the direct-runoff rivers, and perhaps some of the glacier-fed rivers, is a process that can be linked to the age of the catchment. As outlined previously basalts do possess high $^{187}Re/^{188}Os$ (parent/daughter) ratios and will therefore evolve to radiogenic $^{187}Os/^{188}Os$ values in short periods of time. However, taking the average $^{187}Re/^{188}Os$ of Icelandic basalt of ~500 the $^{187}Os/^{188}Os$ ratio would only shift from 0.127 to 0.226 in 12 Myr. Therefore, the variations observed in the dissolved load cannot be simply explained by congruent weathering of basalt.

5.3. Weathering susceptibility and saturation state

The resistance of primary minerals to weathering increases with the degree of sharing of oxygens between adjacent silicon tetraedra in the crystal lattice. The Si–O bond has the highest energy of formation followed by the Al–O bond and even weaker bonds formed between O and other metal cations (such as Na^{2+}, Ca^{2+}, Mg^{2+}) [37]. Thus, amongst the primary basaltic minerals, olivine weathers the most easily because the silicon tetrahedra are only held together by O-metal cations. The stability of primary basalt minerals under the weathering conditions that prevail in Iceland, is not only determined by their dissolution rate but also by the formation of secondary (weathering) minerals and the uptake by biomass. Consumption by secondary minerals and biomass may lower the concentrations of major constituents and maintain undersaturation of the waters with respect to the primary minerals, which as a result continue to dissolve.

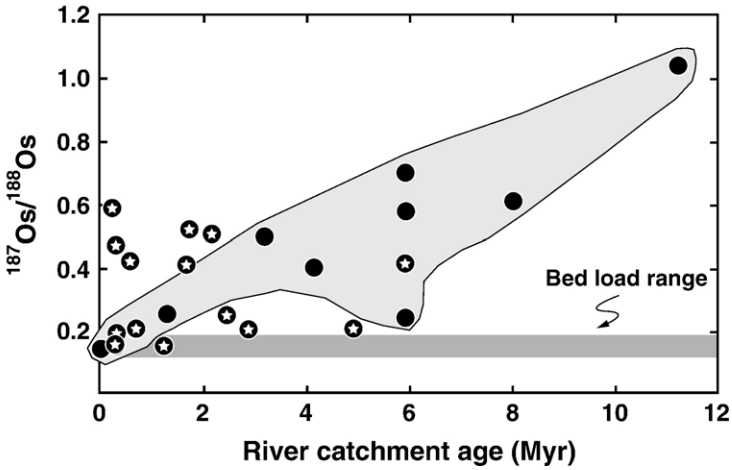

Fig. 7. Dissolved osmium isotope composition versus the catchment river mean age (Myr). The weighted age for each river basin was calculated using the recently updated geological map of Iceland [24]. Non-glacial rivers define a good positive correlation, which indicates that the most radiogenic signatures are observed for the rivers draining old terranes. The radiogenic osmium compositions observed for some of the glacial rivers are unlikely to be the result of an age effect because basaltic phases cannot develop such radiogenic osmium isotope compositions in such a short period of time (<0.6 Myr).

For each river water the stability of primary basaltic minerals can be estimated from the degree of super- and/or understauration in terms of Gibbs free energy (kJ) for the dissolution reaction. The PHREEQC program [38] was used to calculate the saturation state of the waters sampled here relative to the primary basalt minerals. In situ pH and temperature determined in the field, and measured anion and cation concentrations were used for these calculations. The dissociation reactions used are given in the Appendix, and the estimates were made for end-member mineral compositions. The errors on the calculated saturation indices are likely to be within 1–2 log units (cf [38]). These errors arise mainly from uncertainties on the aqueous species dissolution constants and the solubility constants for some minerals. In addition, for those elements preferentially partitioned into organic colloids reported concentrations may be higher than that in the actual dissolved load, although as vegetation and soil cover in Iceland are sparse most rivers are low in organic colloids.

The saturation indices of olivine, clinopyroxene and plagioclase for the samples studied here are shown in Fig. 8, relative to the measured pH. These results indicate that many rivers are significantly undersaturated with

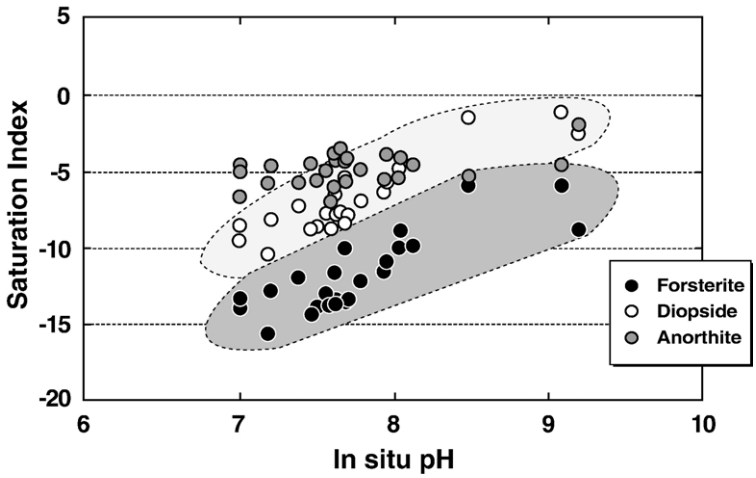

Fig. 8. The water saturation index (SI) of primary basaltic minerals versus the pH of the solution. The SI for the analysed rivers has been calculated by assuming stoichiometric dissolution (see Annex) of primary minerals at low temperature [53]. The degree of under saturation decreases with increasing pH as a result of the strong pH dependence of olivine and diopside solubility.

respect to olivine, clinopyroxene and plagioclase indicating that these phases are unstable and prone to dissolution. For olivine and clinopyroxene the degree of undersaturation decreases with increasing pH, as a result of the strong pH dependence of the solubility of these minerals. The observed range of pH is thought to result largely from two counteracting processes, consumption of protons from mafic mineral and glass dissolution, and generation of protons by uptake of CO_2 from the atmosphere via precipitation and decaying organic matter [19].

In contrast, there is little variation in the saturation index for leached basaltic and rhyolitic glass, which is closer to saturation than the primary end-member minerals in Fig. 8, in all the river waters. The results for hematite and magnetite are not shown but all waters are oversaturated with respect to these phases, indicating that they are stable. Dissolution rates for both minerals and glasses decrease with increasing Si : O ratio, but glass dissolution rates are faster than corresponding mineral rates. The difference between glass and mineral dissolution rates increases with increasing Si : O ratio; ultramafic glasses (Si : O $\leq$ 0.28) dissolve at similar rates to minerals with a similar composition, but Si-rich glasses such as rhyolite (Si : O ~0.4) dissolve $\geq$ 1.6 orders of magnitude faster than corresponding minerals [39].

Dissolution rates of volcanic glasses, olivine, pyroxenes and plagioclase are very dependent on pH. The dissolution rates of olivine and pyroxenes decrease with increasing pH from pH of 2 to 12. However the dissolution rate of plagioclase and volcanic glasses decrease with increasing pH from pH of 2 to about pH 7 but at higher pH the dissolution rates increases [40,41]. Other studies [43,42] suggest that plagioclase and glass dissolution is relatively more important in the young rocks of Iceland where spring fed rivers at high pH dominate than in the old rocks. Both because of the pH effect and simply because of their abundance. The young rocks in the rift zone tend to be more glassy, whereas glass is rare and just confined to the scoria part of the lava flow in the old tertiary rocks.

On the basis of mineral saturation state the weathering susceptibility of the primary basaltic minerals in the rivers studied here are in increasing order; olivine > clinopyroxene > plagioclase > orthopyroxene > magnetite, hematite. These results are in close agreement with previous work on Icelandic rivers and experimental and petrological studies of basalt weathering [44–47]. In the context of the present study they demonstrate that for many of the rivers, some of the primary basaltic-minerals are being preferentially weathered from the host basalt, and incongruent weathering prevails.

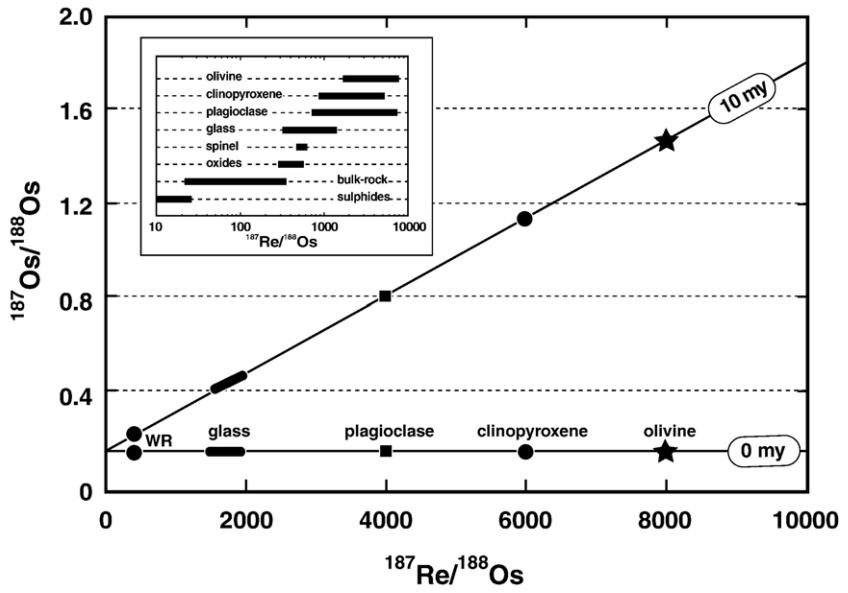

Fig. 9. Hypothetical ^{187}Re–^{187}Os isotope evolution diagram for the constituent minerals of basalt. The silicate phases posses much higher $^{187}Re/^{188}Os$ ratios than bulk-rock or glass, and can produce measurable shifts in the radiogenic isotope ratio after a given time. For example, for an olivine with a $^{187}Re/^{188}Os$ of 8000, the $^{187}Os/^{188}Os$ ratio will evolve from a mantle value of 0.13 to 1.46 in 10 Myr, about 10–16 times the shift observed for bulk rock over the same period of time. Data source for olivine (n=8, [22,48]), for all others, clinopyroxene (n=2, plagioclase (n=5), glass (n=6), spinel (n=2), oxides (n=2), matrix (n=7) and sulphides (n=6) data are from [22] and from A. Gannoun unpublished data.

5.4. The Os isotope signature of primary basaltic minerals

The fractionation of Re and Os during mantle melting and basalt genesis is one of the fundamental processes governing the distribution of these elements in the Earth's crust. Osmium behaves as a compatible element during melting and is preferentially retained in the mantle, whereas Re is moderately incompatible and enters the melt. Thus, mantle-derived basalts have very high Re/Os ratios and their primary minerals crystallise in a high Re/Os environment, and recent work has shown that these phases themselves may fractionate Re/Os even further [22,48]. Fig. 9 illustrates the range of $^{187}Re/^{188}Os$ (parent/daughter) ratios observed in the constituent minerals of basalts. Minerals, such as olivine, pyroxene and plagioclase, possess much higher $^{187}Re/^{188}Os$ ratios than either the bulk-rock or glass, and can produce measurable shifts in the radiogenic isotope ratio on very short timescales (i.e. $\sim 10^6$ years or less). For example, for an olivine with a $^{187}Re/^{188}Os$ ratio of 8000 the $^{187}Os/^{188}Os$ ratio will evolve from a mantle value of 0.13 to 1.46 in 10 Myr, about 10 times the shift observed for bulk rock over the same period of time.

Thus, the primary basaltic phases (olivine, pyroxene and plagioclase) that possess extremely high $^{187}Re/^{188}Os$ ratios are the very same that are significantly undersaturated in many of the Icelandic rivers. Fig. 10 shows the saturation state of the most unstable end members of olivine and clinopyroxene against the measured $^{187}Os/^{188}Os$ isotope ratio for the rivers studied here. For the direct-runoff rivers the waters with the most radiogenic Os isotope composition are also the most highly undersaturated with respect to olivine, clinopyroxene (and plagioclase), suggesting that preferential weathering of these phases is responsible for the Os isotope composition of the dissolved load. Whereas the water samples with low $^{187}Os/^{188}Os$ are those approaching saturation with respect to the these same minerals, indicating that for these catchments weathering is tending towards congruency and the dissolved load approaches that of the bedload (and presumably that of the bedrock itself).

Thus, two key criteria need to be met for basalt weathering to impart a radiogenic Os isotope composition to the dissolved load of rivers. The first is that for the basalt minerals sufficient time must have elapsed for radiogenic growth of ^{187}Os from the decay of ^{187}Re to have occurred. The second is that river waters in the same catchments must be undersaturated with respect to the likely radiogenic basalt minerals, olivine, pyroxene and plagioclase, for their preferential weathering to occur. It might be seen as something of a coincidence that both of these criteria are met for many of the Icelandic rivers, that is that rivers draining older catchments tend to be undersaturated in primary basaltic minerals. However, this most likely reflects the unique geology and structure of Iceland. As outlined previously generally the age of rocks increases with distance from the active volcanic zones. Permeability within the young volcanic zones is higher than the older rocks, and for that reason they have few surface streams. Compaction and sealing by secondary minerals reduces the permeability of the rocks as they move out of the active volcanic zones. As a result direct runoff dominates in the older quaternary and tertiary basalts, whereas a large proportion of the precipitation that falls on the younger volcanic zones

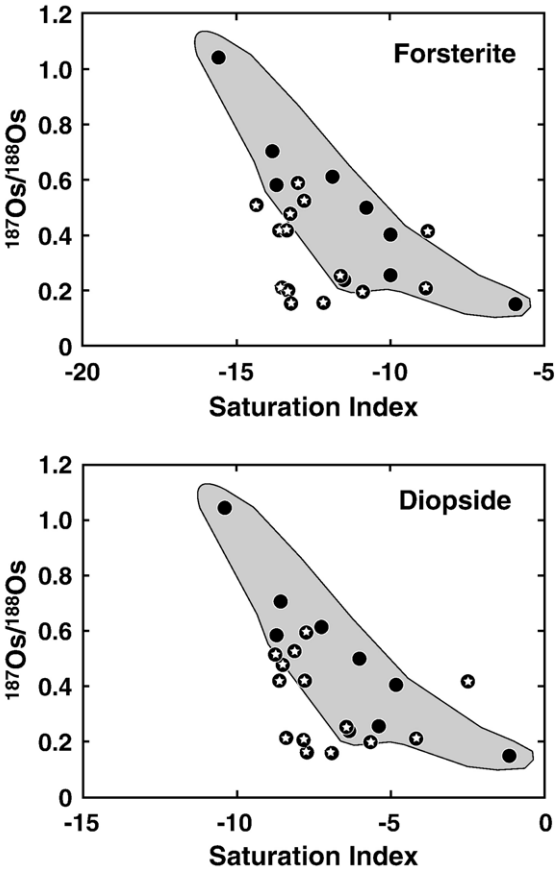

Fig. 10. The dissolved osmium isotope composition versus the saturation index relative to olivine and clinopyroxene. There is a clear covariance between $^{187}Os/^{188}Os$ and SI for non-glacier fed rivers. The most radiogenic samples are the most highly under saturated with respect to the olivine and clinopyroxene. This indicates that the Os isotope composition is dominated by the weathering process for non-glaciers-fed rivers while the glacier fed rivers do not show any relationship (see text).

infiltrates as groundwater that may emerge as springs to feed some rivers. In the groundwaters of the young volcanic zones, limited reaction with mafic silicates will rapidly raise the pH, and hence the waters to saturation, due to the high reactivity of these minerals and the limited supply of acids to the water. In contrast, in the direct-runoff rivers of the older basalt catchments the water will possess a lower pH, and these will be more likely understaurated with respect to the basaltic minerals. It is also probable that there will be a greater proportion of glass in the younger basalts, and rapid dissolution of this glass may act to stabilise the primary basaltic minerals [49]. Whereas, in the older basalts pristine glass is less common, and if it is present is often highly altered. Irrespective of the cause of relationship between catchment age and saturation state, Re–Os isotope data for primary basaltic phases indicate that they can evolve to highly radiogenic compositions on short timescales, and the results presented here indicate that many rivers are undersaturated in the same minerals, which will release this radiogenic Os isotope signal.

5.5. The riverine osmium yield from basaltic terrains

Because mantle-derived basalts usually possess relatively unradiogenic Os isotope compositions it is assumed, not unreasonably, that the riverine Os flux to the oceans from young volcanic terrains will also be unradiogenic. The question then is whether the radiogenic composition of the dissolved load seen in many of the Icelandic rivers could have any significant impact on the riverine Os flux to the oceans.

The proportion of released Os from each river can be estimated using the annual discharge and the total suspended solid. Dissolved osmium accounts for 8–97% (average 45%) of total Os transported by rivers (dissolved and suspended). This range is similar to the proportion of Os mobilised in the Mackenzie river basin (13–69%) [14] or during the weathering of blacks shales (45–90%) [50]. This estimate does not take into account the contribution of the bed load which will decrease the observed range, nor does it consider the possibility of temporal variations in river discharge which might also affect the total suspended load.

It is possible to estimate the entire quantity and isotope composition of the dissolved Os that is supplied to the Atlantic Ocean from Iceland. The rivers studied here (0.01 km^3/yr) account for only some 40% of the annual transport of the suspended load (0.02–0.025 km^3/yr) and their annual discharge (35 km^3/yr) can account for ~21% of the total discharge of the rivers in Iceland (170 km^3/yr) which is about 0.45% of the total world river discharge to the oceans [51]. Dissolved Os from the investigated rivers yields an average Os isotope composition of 0.22 and an annual yield of 0.216 kg/yr which, if representative, translates to 0.98 kg/yr for the whole island. Whereas the Os yield from the suspended load has an average Os composition of 0.16 and an annual yield of 0.202 kg/yr which corresponds to 0.53 kg/yr for the whole of Iceland (Fig. 11). Taking

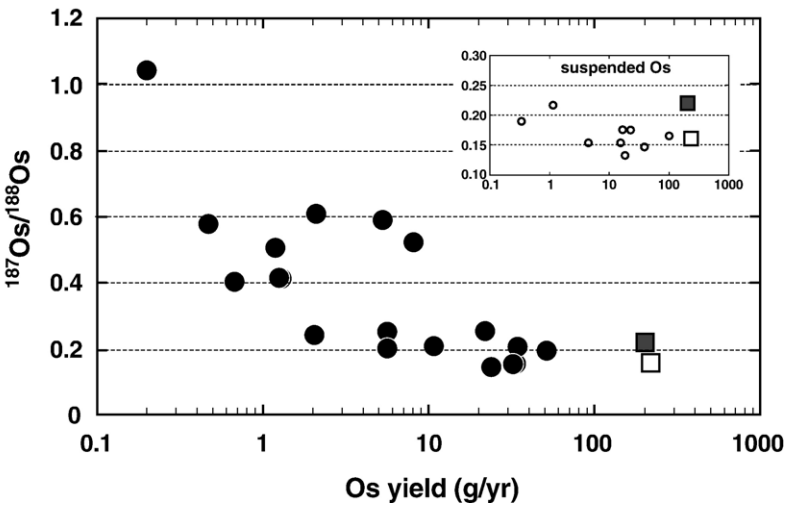

Fig. 11. Dissolved osmium isotope composition versus the Os yield (g/yr) for the Icelandic rivers studied here. Each contribution is calculated using the measured Os concentrations (pg/kg) and the annual mean discharge (km^3/yr) for the given river. The inset graph reports the suspended Os yield and was calculated using the suspended load concentrations (mg/l), Os concentrations (pg/g) and the annual mean discharge (km^3/yr). In both graphs, the filled square denotes the dissolved load whilst the open square denotes suspended load. In both cases Os yield represents the integrated value and the average $^{187}Os/^{188}Os$ ratios.

both dissolved and suspended loads these data indicate that Iceland supplies ~1.5 kg/yr of osmium to seawater with isotopic ratio of 0.200, compared to the global riverine flux estimated to be 300 kg/yr with a $^{187}Os/^{188}Os$ value of 1.54 [26]. Therefore, although the dissolved load is slightly more radiogenic than the suspended load, the overall composition of the material delivered to the ocean is relatively unradiogenic, much lower than the present day seawater value of 1.06. This is simply because rivers with a high annual discharge and unradiogenic $^{187}Os/^{188}Os$ values dominate the Os flux. Simlarly, Os isotope data for basaltic rivers in Java [26] and Papua New Guinea [52] also indicate a relatively unradiogenic Os isotope composition.

6. Concluding remarks

The data presented here indicate that the preferential weathering of basaltic minerals may yield a radiogenic Os isotope signal, although, for relatively young volcanics such as those studied here such effects have a minor impact on the overall riverine signal to the oceans. Nevertheless, for old basaltic terrains, such as continental flood basalts (some of which are in excess of 100 Myr old) their weathering may yield a much more radiogenic Os isotope signal to the Oceans than was previously thought. Similarly, it can be anticipated that incongruent weathering of ancient shield terrains may also impart a highly radiogenic Os isotope composition to seawater (cf [18]).

Acknowledgements

C. Gorge and J. Gaillardet are thanked for major anion analysis performed on the dissolved load at IPG de Paris. We thank B. Schaefer for help with sampling and filtration in the field. This work was supported by the Natural Environment Research Council (under contract NE/B502701/1). We thank H. Elderfield for his express editorial handling and two anonymous reviewers for their comments.

Appendix A

Following Gislason and Arnorsson [49], for an ideal binary solution of a given composition at T and P, the apparent standard state Gibbs free energy of formation,

$$\Delta G^o_{ss}(T,P) = X_i \Delta G^o_i(T,P) + X_j \Delta G^o_j(T,P) + nRT(X_i \ln X_i + X_j \ln X_j)$$

Where ΔG^o_{ss}, ΔG^o_i and ΔG^o_j are the standard-state Gibbs free energy of the solid solution and of pure end-members i and j; X_i and X_j are the corresponding mole fractions of pure-end members i and j; T and P are temperature (K) and pressure of interest (1 atm); R is the gas constant and n is the number of exchange sites per unit cell.

The equilibrium constant (K) is related to the standard Gibbs free energy of reaction at any temperature and pressure by:

$$\Delta G^o(T,P)_r = 2.303\ RT\ \log(Q/K_{ss})$$

Where Q is the reaction quotient of the specific reaction. The saturation index (SI) can be expressed by:

$$SI = \log(Q/K)(T,P).$$

Table A
Dissolution reactions of primary minerals in basalts after [53,39]

Phase	Dissolution reaction	log k	ΔH (kcal)
Forsterite	$Mg_2SiO_4 + 4H^+ \Leftrightarrow 2Mg^{+2} + H_4SiO_4$	28.306	−48.578
Diopside	$CaMgSi_2O_6 + 4H^+ 2H_2O \Leftrightarrow Ca^{+2} + Mg^{+2} + 2H_4SiO_4$	19.894	−32.348
Clino-enstatite	$MgSiO_3 + 2H^+ + H2O \Leftrightarrow Mg^{+2} + H_4SiO_4$	11.342	−20.049
Albite	$NaAlSi_3O_8 + 8H_2O \Leftrightarrow Na^+ + Al(OH)_4^- + 3H_4SiO_4$	−18.002	25.896
Anorthite	$CaAl_2Si_2O_8 + 8H_2O \Leftrightarrow Ca^{+2} + 2Al(OH)_4^- + 2H_4SiO_4$	−19.714	11.58
K-feldspar	$KalSi_3O_8 + 8H_2O \Leftrightarrow K^+ + Al(OH)_4^- + 3H_4SiO_4$	−20.573	30.82
Hydroxyapatite	$Ca_5(PO_4)3OH + 4H^+ \Leftrightarrow 5Ca^{+2} + 3HPO_4^{-2} + H_2O$	−3.421	−36.155
Magnetite	$Fe_3O_4 + 8H^+ \Leftrightarrow 2Fe^{+3} + Fe^{+2} + 4H_2O$	3.737	−50.46
Hematite	$Fe_2O_3 + 6H^+ \Leftrightarrow 2Fe^{+3} + 3H_2O$	−4.008	−30.845
Hekla1 (rhyolitic glass)	$Al_{0.23}SiO_2(OH)_{0.69} + 0.69H+ + 1.31H_2O \Leftrightarrow H_4SiO_4 + 0.23Al^{+3}$	−0.23	
Askja1875 (rhyolitic glass)	$Al_{0.21}SiO_2(OH)_{0.63} + 0.63H^+ + 1.37H_2O \Leftrightarrow H_4SiO_4 + 0.21Al^{+3}$	−0.44	
Hekla Z3 (basaltic glass)	$Al_{0.33}SiO_2(OH)_{0.99} + 0.99H^+ + 1.01H_2O \Leftrightarrow H_4SiO_4 + 0.33Al^{+3}$	0.85	

Appendix B. Supplementary data

Supplementary data associated with this article can be found, in the online version, at doi:10.1016/j.epsl.2006.01.024.

References

[1] J.C.J. Walker, P.B. Hays, J.F. Kasting, A negative feedback mechanism for the long term stabilization of the earth's surface temperature, J. Geophys. Res. 86 (1981) 9776–9782.

[2] R.A. Berner, A.C. Lasaga, R.M. Garrels, The carbonate–silicate geochemical cycle and its effect on atmospheric carbon dioxide over the past 100 million years, Am. J. Sci. 283 (1983) 641–683.

[3] M.E. Raymo, W.F. Ruddiman, P.N. Froelich, Influence of late Cenozoic mountain building on ocean geochemical cycles, Geology 16 (1988) 649–653.

[4] R.L. Armstrong, Glacial erosion and the variable isotopic composition of strontium in sea water, Nature 230 (1971) 132–133.

[5] J. Quade, L. Roe, P.G. DeCelles, T.P. Ojha, The Late Neogene $^{87}Sr/^{86}Sr$ record of lowland Himalayan rivers, Science 276 (1997) 1828–1831.

[6] F.M. Richter, K.K. Turekian, Simple models for the geochemical response of the ocean to climatic and tectonic forcing, Earth Planet. Sci. Lett. 119 (1993) 121–131.

[7] K.W. Burton, D. Vance, Glacial–interglacial variations in the neodymium isotope composition of seawater in the Bay of Bengal recorded by planktonic foraminifera, Earth Planet. Sci. Lett. 176 (2000) 425–441.

[8] W.J. Pegram, S. Krishnaswami, G.E. Ravizza, K.K. Turekian, The record of sea water $^{187}Os/^{186}Os$ variation through the Cenozoic, Earth Planet. Sci. Lett. 113 (1992) 569–576.

[9] B. Peucker-Ehrenbrink, G. Ravizza, A.W. Hofmann, The marine $^{187}Os/^{186}Os$ record of the past 80 million years, Earth Planet. Sci. Lett. 130 (1995) 155–176.

[10] R. Oxburgh, Residence time of osmium in the oceans, Geochem. Geophys. Geosyst. 2 (2001) (2000GC000104).

[11] S. Levasseur, J.-L. Birck, C.J. Allègre, Direct measurement of femtomoles of osmium and the $^{187}Os/^{188}Os$ ratio in seawater, Science 282 (1998) 272–274.

[12] B. Peucker-Ehrenbrink, G. Ravizza, The marine osmium isotope record, Terra Nova 12 (2000) 205–219.

[13] S. Levasseur. Contribution a l'etude du cycle externe de l'osmium, Ph.D., IPGP, 1999.

[14] Y. Huh, J.L. Birck, C.J. Allègre, Osmium isotope geochemistry in the Mackenzie River basin, Earth Planet. Sci. Lett. 222 (2004) 115–129.

[15] A. Stefánsson, S.R. Gíslason, S. Arnórsson, Dissolution of primary minerals in natural waters II. Mineral saturation state, Chem. Geol. 172 (2001) 251–276.

[16] F.V. Blanckenburg, T. Nägler, Weathering versus circulation-controlled changes in radiogenic isotope tracer composition of the Labrador Sea and North Atlantic Deep Water, Paleoceanography 16 (2001) 424–434.

[17] T. van de Flierdt, M. Frank, D.C. Lee, A.N. Halliday, Glacial weathering and the hafnium isotope composition of seawater, Earth Planet. Sci. Lett. 198 (2002) 167–175.

[18] B. Peucker-Ehrenbrink, J.D. Blum, Re–Os isotope systematics and weathering of Precambrian crustal rocks: implications for the marine osmium isotope record, Geochim. Cosmochim. Acta 62 (1998) 3193–3203.

[19] S.R. Gíslason, H.P. Eugster, Meteoric water-basalt interactions: I. A laboratory study, Geochim. Cosmochim. Acta 51 (1987) 2827–2840.

[20] C. Dessert, B. Dupré, J. Gaillardet, L.M. François, C.J. Allègre, Basalt weathering laws and the impact of basalt weathering on the global carbon cycle, Chem. Geol. 202 (2003) 257–273.

[21] G. Ravizza, B. Peucker-Ehrenbrink, Chemostratigraphic evidence of Deccan volcanism from the marine osmium isotope record, Science 302 (2003) 1392–1395.

[22] A. Gannoun, K.W. Burton, L.E. Thomas, I.J. Parkinson, P.V. Calsteren, P. Schiano, Osmium isotope heterogeneity in the constituent phases of mid-ocean ridge basalts, Science 303 (2004) 70–72.

[23] S. Moorbath, H. Sigurdsson, R. Goodwin, K–Ar ages of the oldest exposed rocks in Iceland, Earth Planet. Sci. Lett. 4 (1968) 197–205.

[24] H. Jóhannesson, K. Saemundsson, Tectonic map of Iceland 1:500,000, Icelandic Institute of Natural History, Reykjvík, Iceland, 1998.

[25] S.R. Gíslason, S. Arnórsson, H. Ármannsson, Chemical weathering of basalt in southwest Iceland: effects of runoff, age of rocks and vegetative/glacial cover, Am. J. Sci. 296 (1996) 837–907.

[26] S. Levasseur, J.-L. Birck, C.J. Allègre, The osmium riverine flux and the oceanic mass balance of osmium, Earth Planet. Sci. Lett. 174 (1999) 7–23.

[27] J.-L. Birck, M. Roy-Barman, F. Capmas, Re–Os isotopic measurements at femtomole level in natural samples, Geostand. Newsl. 20 (1997) 19–27.

[28] R.A. Creaser, D.A. Papanastassiou, G.J. Wasserburg, Negative thermal ion mass spectrometry of osmium, rhenium and iridium, Geochim. Cosmochim. Acta 55 (1991) 397–401.

[29] J.W. Völkening, T. Walczyk, K. Heumann, Osmium isotope ratio determination by negative thermal ionisation mass spectrometry, Int. J. Mass Spectrom. Ion Process. 105 (1991) 147.

[30] S.B. Shirey, R.J. Walker, The Re–Os isotope system in cosmochemistry and high-temperature geochemistry, Annu. Rev. Earth Planet. Sci. 26 (1998) 423–500.

[31] E.H. Hauri, S.R. Hart, Re–Os isotope systematics of HIMU and EMII oceanic island basalts from the south Pacific Ocean, Earth Planet. Sci. Lett. 114 (1993) 353–371.

[32] J.M. Luck, C.J. Allègre, ^{187}Re–^{187}Os systematics in meteorites and cosmochemical consequences, Nature 302 (1983) 130–132.

[33] I.V. Zander, G. Brügmann, A.W. Hofmann, D. McKenzie, D.F. Mertz. Osmium isotope signatures of picrites and basalts from Theistareykir (North Iceland), Goldschmidt, Oxford, Cambridge Publications 5 (2000) 1034.

[34] Y. Smit. The Snæfellsnes transect: a geochemical cross-section through the Iceland plume, Ph.D., The Open University, 2001.

[35] A.C. Skovgaard, M. Storey, J. Baker, J. Blusztajn, S.R. Hart, Osmium–oxygen isotopic evidence for a recycled and strongly depleted component in the Iceland mantle plume, Earth Planet. Sci. Lett. 194 (2001) 259–275.

[36] E.K. Berner, R.A. Berner, Global Environment: Water, Air and Geochemical Cycles, Prentice Hall, Upper Saddle River, New Jersey, 1996. 376 pp.

[37] E.H. Oelkers, General kinetic description of multioxide silicate mineral and glass dissolution, Geochim. Cosmochim. Acta 55 (2001) 2779–3703.

[38] D.L. Parkhurst, C.A.J. Appelo, User's guide to PHREEQC (Version2)-A computer program for speciation, batch-reaction, one-dimensional transport and inverse geochemical calculations, USGS Water-Resources Invest. Rep. 99-4259, 1999, 310 pp.

[39] D. Wolff-Boenisch, S.R. Gíslason, E. H Oelkers, C.V. Putnis, The dissolution rates of natural glass as a function of their composition at pH 4 and 10.6, and temperatures from 25 to 74 °C, Geochim. Cosmochim. Acta 68 (2004) 4843–4858.

[40] G.S. Pokrovski, J. Schott, Kinetic and mechanism of forsterite dissolution at 25 °C and pH from 1 to 12, Geochim. Cosmochim. Acta 64 (2000) 3313–3325.
[41] E.H. Oelkers, J. Schott, An experimental study of enstatite dissolution rates as a function of pH, temperature, and aqueous Mg and Si concentration, and the mechanism of pyroxene/pyroxenoid dissolution, Geochim. Cosmochim. Acta 65 (2001) 1219–1231.
[42] S.R. Gíslason, E.H. Oelkers, Mechanism, rates, and consequences of basaltic glass dissolution: II. An experimental study of the dissolution rates of basaltic glass as a function of pH and temperature, Geochim. Cosmochim. Acta 64 (2003) 3817–3832.
[43] A.E. Blum, L.L. Stillings, Chemical weathering of feldspars, in: A.F. White, S.L. Brantley (Eds.), Chemical Weathering Rates of Silicate Minerals, Rev. Min., vol. 31, 1995, pp. 291–351.
[44] S.S. Goldich, A study on rock weathering, J. Geol. 46 (1938) 17–58.
[45] R.A. Eggelton, C. Foudoulish, D. Farkevisser, Weathering of basalts: changes in rock chemistry and mineralogy, Clays Clay Miner. 35 (1987) 161–169.
[46] J.F. Banfield, B.F. Jones, D.R. Veblen, An AEM-TEM study of weathering and diagenesis, Abert Lake, Oregon: I. Weathering reactions in the volcanics, Geochim. Cosmochim. Acta 55 (1991) 2781–2793.
[47] H.W. Nesbitt, R.E. Wilson, Recent chemical weathering of basalts, Am. J. Sci. 292 (1992) 740–777.
[48] K.W. Burton, A. Gannoun, J.-L. Birck, C.J. Allègre, P. Schiano, R. Clocchiatti, O. Alard, Rhenium–osmium compatibility in olivine and the consequences for terrestrial basalt chemistry, Earth Planet. Sci. Lett. 198 (2002) 63–76.
[49] S.R. Gíslason, S. Arnórsson, Saturation state of natural waters in Iceland relative to primary and secondary minerals in basalts, in: R.J. Spencer, I.M. Chou (Eds.), Fluid–Mineral Interaction, Geochemical Society, Special Publication, vol. 2, 1990, pp. 373–393.
[50] B. Peucker-Ehrenbrink, R.E. Hannigan, Effects of black shale weathering on the mobility of rhenium and platinum group elements, Geology 28 (2000) 475–478.
[51] A. Baumgartner, E. Reichel. The world water balance, Amsterdam, Elsevier Scientific Publishing Company, 179 pp.
[52] C.E. Martin, B. Peucker-Ehrenbrink, G.J. Brunskill, R. Szymczak, Sources and sinks of unradiogenic osmium runoff from Papua New Guinea, Earth Planet. Sci. Lett. 183 (2000) 261–274.
[53] S.R. Gíslason, S. Arnórsson, Dissolution of primary basaltic minerals in natural waters: saturation and kinetics, Chem. Geol. 105 (1993) 117–135.